Assessment of reproductive toxicity of Cyfluthrin and Pestban either individually or combined in adult male albino rats

Heba El-Sayed Mostafa[1,2], Eman A. Alaa El-Din[2], Eman M. Kamel[3], Shimaa A. Fareed[3]

[1] Al-Rayan National College of Medicine, Al Medina, Saudi Arabia

[2] Department of Forensic Medicine & Clinical Toxicology, Faculty of Medicine, Zagazig University, Egypt

[3] Department of Anatomy & Embryology, Faculty of Medicine, Suez Canal University, Ismailia, Egypt

SUMMARY

Many studies on individual pesticide risk assessments are available, but the toxicity of combined usage is still to estimate. So, the current study investigated reproductive toxicity induced by exposure to cyfluthrin (CYF) and pestban (PES) and their mixture in adult male albino rats. Forty adult male albino rats were randomized into four groups. All treatments were given daily by oral gavage for 60 days. Group I (control group): this group included 16 rats, divided into two equal subgroups: subgroup Ia (negative control) and subgroup Ib (a vehicle control), in which each rat received 2 ml of corn oil. Group II: CYF group (15.6 mg/kg). Group III; PES group (7.45 mg/kg). Group IV: CYF + PES. Individual CYF and PES exposure significantly decreased testicular weight, serum testosterone level, and epididymal sperm count when compared to the control group. These biochemical changes were confirmed by histological and ultra-structural disarray and reduced immunoreactions of Melan-A (also known as MART-1, Melanoma Antigen Recognized by T-cells), but mutual exposure to both pesticides resulted in a highly significant difference compared to other treated groups. Co-administration of CYF and PES aggravated testicular toxicity, exhausting the endogenous antioxidant status, and down-regulating the immune expression of Melan-A. So, mixing both components can intensify the damaging effects of each compound on testes.

Keywords: Cyfluthrin – Pestban – Testicular toxicity – Rats

INTRODUCTION

Nowadays, farming activities are highly contingent on pesticide use. The pesticide's use play has brought considerable benefits in increasing the availability and food quality by playing an essential role in the expansion of agriculture by decreasing the loss of crops and promoting yield, in addition to enhancing public health in general. Nevertheless, either overuse or misuse of pesticides leads to a great range of negative consequences to species diversity, the environment, and the health of both animals and humans, as is well reported in numerous toxicological studies (Silva et al., 2022).

Corresponding author:
Shimaa Antar Fareed. Department of Anatomy & Embryology, Faculty of Medicine, Suez Canal University, Ismailia, Egypt. E-mail: Shimaa.anter.79@gmail.com - ORCID ID: https://orcid.org/0000-0002-7780-3317

Submitted: February 26, 2023. **Accepted:** May 26, 2023

https://doi.org/10.52083/MMCK6104

The improper application of these pesticides can produce health problems, neurodegenerative diseases, reproductive toxicity, carcinogenicity, and perturbation of the endocrine system (Mohammadi et al., 2021). The widespread resistance and toxicological influence of hazardous pesticides pose unreceptive results on different environmental species and humans, straightforwardly by bioaccumulation or indirectly through the food chain.

Pesticide residues constantly present above permissible legal levels in diversified forms, so much attention has happened likely to regulate their usage without maleficence or negatively affecting the environment (Parra-Arroyo et al., 2022).

Following the World Health Organization reports, the intoxication of pesticides presents a foremost community and public health question; about 3 million cases of pesticide toxicity happen yearly, killing almost 250-370,000 individuals (Kamande et al., 2022).

β-Cyfluthrin (CYF), a class II Pyrethroid (PYR), is an insecticide used worldwide in farming, gardening, and household applications. Repeatedly it is used in veterinary medicine, farming against various pests, and residential and industrial settings. Studies explaining mechanisms of reproductive toxicity regarding this insecticide are limited (Wang et al., 2022).

Pestban (PES) is an organophosphorus (OP) insecticide containing 48% chlorpyrifos (CPF). It is used widely in many agricultural practices; against plants and pests to control animal ectoparasites, although CPF is known as a neurotoxicant through cholinesterase inhibition. Inclusive data assessing pestban effects on gestational length, reproduction, and fertility parameters of males and females are still not clear enough and limited (Morgan and El-Aty, 2008).

The marketing of PYR and OP mixes propagates widely in developing countries and has increased toxicity predominance**.** Trials to prophesy toxicity related to mixtures depending on individual chemicals' acquaintance commonly led to false and deficient conclusions. The interaction due to mixing two or more pesticides is not always expected, because this combination may have summative, potentiating collusive, or inhibitory effects (Alaa El-Din et al., 2022). Therefore, this study assessed testicular toxicity caused by individual and mutual exposure to cyfluthrin and pestban in adult albino rats.

MATERIALS AND METHODS

Chemicals

β-*Cyfluthrin*: it was manufactured by Sigma-Aldrich Company, Louis St., USA, and bought from Sigma Egypt.

Pestban: it was obtained from Indora (Italian company).

Corn oil: it was bought from Sekem Co. in Cairo, Egypt, (a vehicle for both insecticides)

Animals

This study was acted upon at the animal house of the Faculty of Medicine, Suez Canal University, Egypt. Forty adult male albino rats aged two months and ranging in weight from 150 to 170 grams, were used in the present study. The rats were purchased from the Faculty of Veterinary Medicine Animal House, Suez Canal University, Egypt. Rat food and water were freely available to the rodents in the breeding facility. The rats were kept in filter-top plastic cages in a room with artificial lighting and temperature control (23 ±1 °C). The procedure of the experiment was done according to the National Institute of Health Guidelines for the Care and Use of Laboratory Animals (NIH Publications No. 8023, revised 1978). The protocol of the study was confirmed by the Suez Canal University Faculty of Medicine's Research Ethics Committee. (Egypt) (Research Number: 5072#) on Oct 18, 2022.

Experimental design

The total male rats were randomly divided into four groups. The experiment lasted sixty days, and all groups received supplements by oral gavage each day.

Group I (control group): This group included 16 rats, and was divided into two equal subgroups:

Subgroup Ia (negative control): Each rat in this group received a regular diet and water for 60 days. These groups were used as reference comparable values.

Subgroup Ib (positive control): Each rat received 2 ml of corn oil (vehicle of CYF and PES).

Group II (β-Cyfluthrin group) (eight rats): Each rat was treated with CYF at a daily dose of 15.6 mg/kg b.w./day (1/20 of oral LD50) (LD 50 = 380 mg/kg b.w./day) according to Mohafrash et al. (2017).

Group III (Pestban group) (eight rats): Each rat received PES at a daily dose of 7.45 mg/kg b.w./day (1/20 of the oral LD50) (Morgan and El-Aty, 2008), (Abd-Elhakim et al., 2021).

Group IV (Cyfluthrin + Pestban) (eight rats): Each rat received CYF+PES for 60 days (using the same previously mentioned doses and same exposure time).

After exposure to CYF and PES for 60 days, an intraperitoneal injection of thiopental (50 mg/kg) was used to anaesthetize the rats of all groups (Nagaya et al., 2004). In accordance with Nemzek et al. (2001), samples of blood were taken from the retroorbital venous plexus; then scarification of rats was performed. In order to preserve blood samples for hormonal examination, they were kept at -80 °C. Physiological saline was used to swiftly remove the testes, remove any adhering tissue, wash them, and dry them.

Body and testis weight measuring

A digital balance was used to weigh the rats before they were anaesthetized and sacrificed. Testes were removed and weighed, and organ/somatic index were calculated. The relative testes weight = Absolute testes weight/ Whole body weight ×100 (Hamoud, 2019).

Hormonal study

Solid phase radioimmunoassay method was used to measure serum testosterone levels (Kim et al., 2012), while enzyme-linked immunosorbent assay (ELISA) was used to measure serum rat luteinizing hormone (LH) and follicular stimulating hormone (FSH) levels (Chen et al., 2015).

Measurement of blood levels of oxidative stress biomarkers:

Total antioxidant capacity (TAC) was evaluated by using the colorimetric technique following the method described by (Koracevic, 2001). Glutathione peroxidase (GPx), reduced glutathione (GSH), and malondialdehyde (MDA) were measured according to the methods described by Zhang et al. (2018), Ensafi et al. (2008) and Aini et al. (2022), respectively.

Epididymal spermatozoan examination:

Spermatozoa were collected according to Mostafa et al. (2016), epididymal content of every rat was obtained immediately by cutting the tail of the epididymis and squeezing it gently to gain the sparkling of freshly undiluted semen in a clean Petri dish and incubated at 37 °C for half of an hour for liquefaction then we started to proceed the following examinations; sperm count, motility of sperms, and epididymal sperm viability were studied and estimated according to the method reported by Adamkovicova et al. (2016). Then, the percentage of epididymal sperm abnormalities (abnormal forms) was calculated following Vasan (2011), and the sperm abnormal forms were described according to Mori's classification, who classified abnormal sperms into deformed heads and tails (tailless and deformed) (Mori et al., 1991).

Histopathological examination

Testes were preserved in 10% formalin solution, then dehydrated, cleared in xylene, fixed, and blocked-in paraffin using an automatic tissue processor. Five micrometers thick sections were cut by a rotary microtome and stained by the hematoxylin & eosin (H&E) and PAS stains (Hsu, 2015).

Ultrastructural study

Specimens from the testes for electron microscopy examination were promptly fixed in 2.5% phosphate-buffered glutaraldehyde (pH 7.4), post-fixed in 1% osmium tetroxide in the same buffer at 4°C, dehydrated and fixed in epoxy resin. Leica Ultracut UCT was used to create ultrathin slices that were then stained with uranyl acetate,

and lead citrate (Van der Horst et al., 2019), seen using a JEOL JEM 1010 electron microscope and captured on camera (Jeol Ltd, Tokyo, Japan) in the Histology and Cell Biology Department, Faculty of Medicine, Al-Azhar University (Egypt).

Immunohistochemical examination

The sections of testis were stained with monoclonal antibodies targeting Melan-A by the avidin-biotin-peroxidase complex (ABC) kit. The sections were then deparaffinized, rehydrated, trypsinized (1 mg pronase/mL Tris-buffered saline), treated with 3% H_2O_2 for 30 minutes at room temperature, and then washed three times. After then, the slices were exposed to primary antibodies for an additional hour. ABC was incubated for 30 minutes following the second antibody infusion. Complete cleaning with Tris-buffered saline (pH: 7.4) was performed on the sections (Shojaeepour et al., 2021).

Statistical analysis

The mean and standard deviation of the data for all groups were displayed (X ± SD). The collected data were handled and analyzed using the SPSS program (SPSS Inc., 2007). One-way analysis of variance was used to find statistically significant differences (ANOVA), followed by the LSD test for multiple comparisons between the different groups. The percentage was assessed by the chi-square test. The test results were considered significant when p value <0.05. P-value <0.01, and <0.001 were considered highly significant.

RESULTS

Effects on body weight and testis weight

The present study showed that mean values of the final body weight and testicular weight (absolute and relative) in CYF (II) and PES (III) treated groups had significantly decreased compared to the control group, but they showed high significant decreases (p-value <0.01) in combined (CYF+PES) treated group (group IV) compared to other studied groups (Table 1).

Hormonal study

Table 2 showed that serum testosterone was significantly reduced in rats individually exposed to CYF and PES, and highly significantly reduced in combined CYF+PES-treated group (group IV). Serum levels of both LH &FSH were significantly decreased in CYF and PES groups; p-value <0.05, where more decrease was noticed in the combined group IV; p-value <0.01 compared with control groups.

Blood levels of oxidative stress biomarkers

Total antioxidant capacity (TAC), glutathione peroxidase (GPx), and reduced glutathione (GSH) were reduced in group-II and group-III treated rats, and were highly significantly reduced in combined treated groups. While Malondialdehyde (MDA) was significantly increased in rats individually exposed to CYF, PES was highly significantly increased in the mutually treated group (Table 3).

Table 1. Initial body weight, final body weight, absolute testis weight and relative testis weight in the study groups.

	Control groups		CYF	PES	CYF + PES
	Ia	Ib			
Initial body weight (g)	189.17± 6.61	188.67± 5.23	189.53± 3.71	190.75 ±8.27	190.23± 6.81
Final body weight (g)	217.83± 5.11	217.59± 7.44	184.83± 4.34*	183.96± 5.62*	160.17± 4.83**#
Absolute testis weight (g/100 g final body weight)	1.77± 0.06	1.76± 0.076	0.95 ±0.052*	0.89± 0.065*	0.660± 0.032**#
Relative testis weight (g)	0.721± 0.03	0.730± 0.05	0.524 ±0.07*	0.500± 0.09*	0.314± 0.08**#

The relative testis weight of each animal is calculated according to the formula:
Relative testis weight = Absolute weight (g) * 100
Final body weight
* p < 0.05 vs control groups
** p < 0.01 vs control groups
# p < 0.05 vs groups II & III

Table 2. Serum testosterone (ng/ml), FSH (ng/ml), and LH (mIU) of adult albino rats among the studied groups.

	Control groups		CYF	PES	CYF + PES
	Ia	Ib			
Testosterone (ng/ml)	1.67 ± 0.49	1.69 ± 0.35	0.86 ± 0.35*	0.90 ± 0.37*	0.25 ± 0.04**#
FSH (ng/ml)	5.96 ± 1.99	6.12 ± 0.32	3.76 ± 2.32*	4.12 ± 1.01*	3.00 ± 0.23**#
LH (mIU)	9.42 ± 1.79	9.37 ± 1.43	6.001 ± 1.62*	5.98 ± 1.39*	3.11 ± 0.89**#

* p < 0.05 vs control groups
** p < 0.01 vs control groups
# p < 0.05 vs groups II & III

Table 3. Oxidative stress and apoptosis biomarkers in the testis homogenates of the study groups: Total antioxidant capacity (TAC), Glutathione peroxidase (GPx), Reduced glutathione (GSH) and Malondialdehyde (MDA).

	Control group		CYF	PES	CYF + PES
	Ia	Ib			
TAC (mmol/g protein)	0.99 ± 0.005	0.97 ± 0.005	0.68 ± 0.003*	0.65 ± 0.012*	0.38 ± 0.016**
GPx (ng/mg protein)	144.17 ± 4.37	144.06 ± 5.46	130.23 ± 3.09*	131.21 ± 2.07*	115.23 ± 3.09**#
GSH (mmol/ g protein)	3.89 ± 0.01	3.99 ± 0.04	2.39 ± 0.02*	2.46 ± 0.03*	1.77 ± 0.01**#
MDA (nmol/g protein)	11.31 ± 0.04	10.99 ± 0.07	14.1 ± 0.21*	15.3 ± 0.45*	18.4 ± 0.57**#

* p < 0.05 vs control groups
** p < 0.01 vs control groups
# p < 0.05 vs groups II & III

Epididymal spermatozoa

Normal sperm morphology by Giemsa staining showed a normal head, normal mid-piece, and normal straight tail (Fig. 1a). Sperms of Cyfluthrin treated group showed abnormally polygonal heads, a missing middle piece with a very thin tail (Fig. 1b), while sperms of the Pestban treated group showed different shapes of heads either small oval, bent shape heads or absences of heads, with a detached tail (Fig. 1c). Sperms of combined Cyfluthrin & Pestban treated group showed absent heads, eroded midpiece, and irregular tail (Fig. 1d). Abnormal morphology of sperms in the study groups were described in Chart 1.

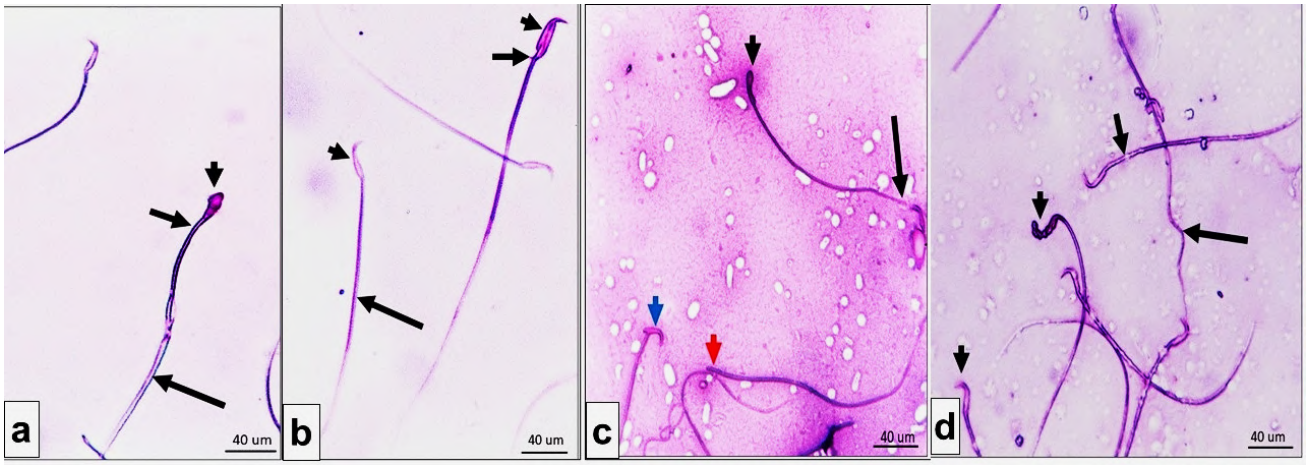

Fig. 1.- Sperm morphology in Giemsa staining **(a):** Normal sperm with normal head (arrowhead), normal midpiece (short head), and normal straight tail (long arrow). **(b):** Sperms of Cyfluthrin-treated group show abnormally polygonal heads (arrowheads), missing middle piece (short arrow) with very thin tail (long arrow). **(c):** Sperms of Pestban-treated group show different shapes of heads either small oval (black arrowhead), bent shape head (blue arrowhead), or absences of the head (red arrow head), with a detached tail (long arrow). **(d):** Sperms of combined Cyfluthrin-and-Pestba- treated group show absent heads (arrowheads), eroded midpiece (short arrow), and irregular tail (long arrow). Giemsa ×400. Scale bars = 40 µm.

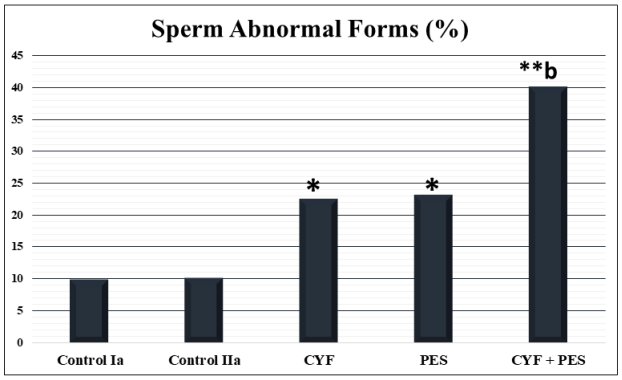

Chart -1 showing; the percent of sperm abnormal forms of the study groups. * $p < 0.01$ vs control groups. ** $p < 0.001$ vs control groups. **b** $p < 0.001$ vs groups II & III

The mean value of sperm motility, viability, and count of the CYF group (II), PES group (III), and combined treated group (IV) showed a highly significant reduction when compared to those in the control group. Additionally, rats treated with pesticides (groups II and III) substantially (p 0.05) had higher mean values of sperm head abnormalities than rats in the control group. While rats in the CYF + PES group (IV) showed the highest significant difference ($p < 0.01$) when compared to those of control and individual CYF- and PES-treated groups (II and III). All data were expressed in (Table 4) and (Chart 2).

Histopathological results

H&E staining

The testicular tissue of the control group showed normal-shaped seminiferous tubules, some with patent lumina, but others showed aggregation of sperms. They were separated by narrow interstitial cells containing Leydig cells and blood vessels (Fig. 2a). Myoid cells and all spermatogenic cell phases were present in the majority of the seminiferous tubules (Fig. 2b).

The testicular parenchyma of the Cyfluthrin-treated group (II) showed irregularly shaped seminiferous tubules, mostly showing a separation of germinal epithelium, irregularly arranged germinal cells, or empty seminiferous tubules. Thickened & edematous interstitial tissues with very dilated and congested blood vessels were noted (Fig. 3a). The primary spermatocytes were either destructed or collected near the center. The secondary spermatocytes were found near the center, and some spermatids were noticed near the basement membrane or irregularly distributed (Fig. 3b).

Table 4. Sperm count, motility, viability, and abnormal forms.

	Control		CYF	PES	CYF + PES
	Ia	IIa			
Sperm count (/ml)	92.55 ±3.55	91.73± 4.57	53.02 ± 7.4*	55.00 ± 6.1*	40.66± 11.83**a
Sperm motility %	73.65 ± 22.4	73.46 ± 51.1	57.74 ± 13.3#	56.99 ± 27.2#	32.42 ± 14.9*a
Sperm viability %	79.12 ± 23.4	78.32 ± 22.5	47.77 ± 12.1#	47.54 ± 23.5#	30.56 ± 15.4**a
Sperm abnormal forms (%)	9.98 ± 1.79	10.15 ± 2.33	22.50 ± 2.15*	23.21 ± 1.33*	40.10 ± 4.21** b

* $p < 0.01$ vs control groups
** $p < 0.001$ vs control groups
# $p < 0.05$ vs control groups
a $p < 0.05$ vs groups II & III
b $p < 0.001$ vs groups II & III

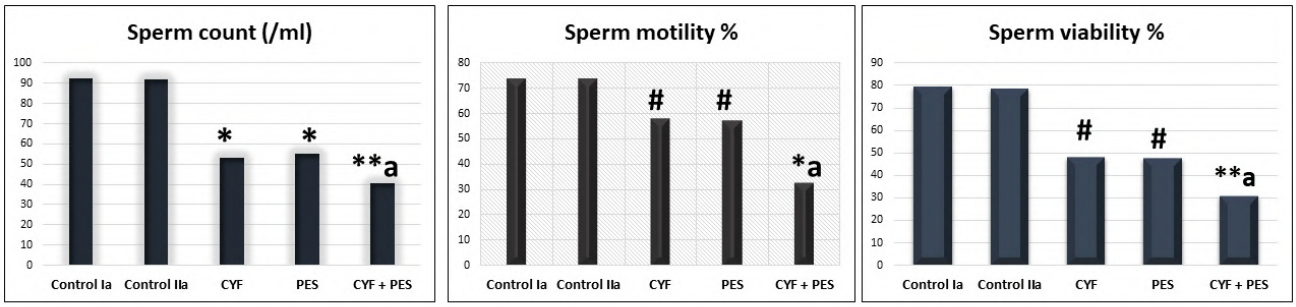

Chart-2 showing; the mean sperm count, percent of motility and viability.
* $p < 0.01$ vs control groups. ** $p < 0.001$ vs control groups. # $p < 0.05$ vs control groups. **a** $p < 0.05$ vs groups II & III

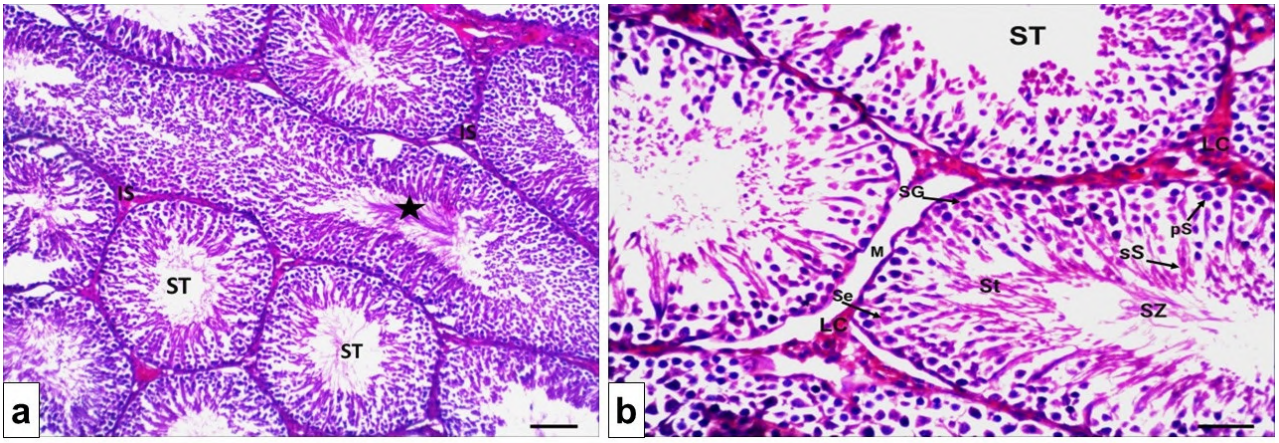

Fig. 2.- Testicular tissue of a rat from the control group showing **(a):** The testicular parenchyma contains seminiferous tubules (ST), some of their lumina were patent, but some showed aggregation of sperms (star). Seminiferous tubules are separated by narrow interstitial cells (IS). **(b):** Each seminiferous tubule contains the myoid cells (M), spermatogonia (SG), Sertoli cells (Se), primary spermatocytes (pS), secondary spermatocyte (sS), and elongated spermatids (St) and spermatozoa (SZ). Leydig cells in the interstitial tissues (LC). H&E staining. Scale bars: a = 40 µm (x200) and b = 20 µm (x400).

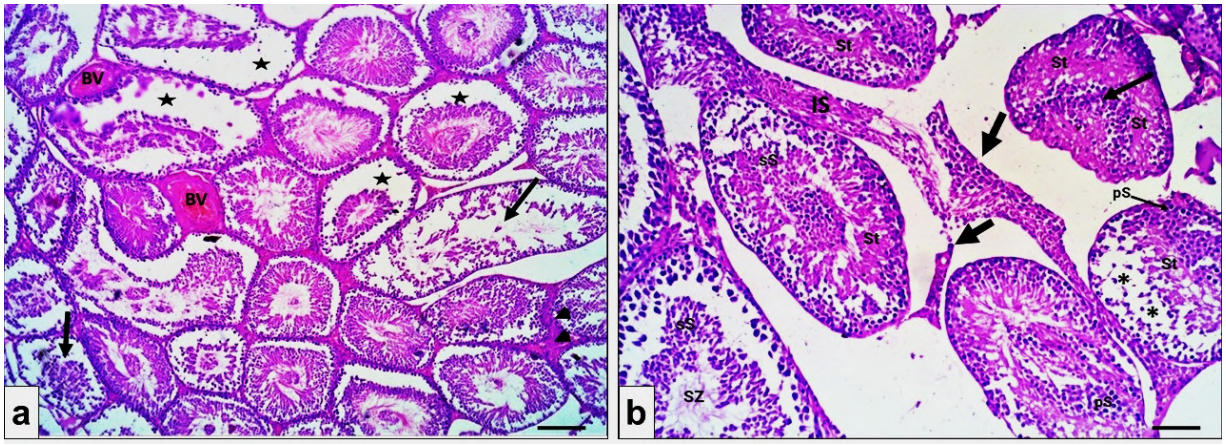

Fig. 3.- Testicular tissue of a rat from the Cyfluthrin-treated group showing **(a):** The testicular parenchyma contains irregularly shaped seminiferous tubules, mostly showing the separation of germinal epithelium (star) or irregularly arranged germinal cells (arrow). Thickened and congested interstitial tissues (arrowheads) with very dilated and congested blood vessels (BV). **(b):** The seminiferous tubules show great irregularity in the arrangement of germinal cells. The primary spermatocytes either destructed (arrow) or (pS) near the center, the secondary spermatocytes (Ss) near the center, and some spermatids (St) lie near the basement membrane or are irregularly distributed. Some tubules show normal spermatozoa (Sz) in their lumen. Others show empty spaces (*). Notice dilated interstitial tissues (IS) or destructed (short arrows). H&E staining. Scale bars: a = 40 µm (x200) and b = 20 µm (x400).

The testicular parenchyma of Pestban-treated group (III) showed a loss of interstitial spaces. Various components of seminiferous tubules were either normal, irregularly distributed tissues or destructed with linear germinal cells inning the basement membrane (Fig. 4a). Some tubules showed separation of germinal cells and were lined by thick capsule with subscapular separation of tissues and very dilated subscapular blood vessels. Some seminiferous tubules showed a collection of germinal cells at the center and spermatids near the center. The interstitial tissues showed infiltration and exudation (Fig. 4b).

The testicular parenchyma of the combined Pestban- and Cyfluthrin-treated group (IV) were lined by a very thick capsule with subscapular separation, exudation, and congested blood vessels. The interstitial tissues showed exudation and congested and dilated blood vessels (Fig. 5a). The seminiferous tubules showed separation of germinal cells from the basement membrane with a central collection of different germ cells (Fig. 5b). Some tubules showed intralaminar hemorrhages and necrotic areas (Fig. 5c). The Spermatogonia were condensed and enlarged. The primary spermatocytes were enlarged with pericellular space and few in number. Secondary spermatocytes were irregular in shape, linearly arranged, or collected in rows. Most of the spermatids were small (Fig. 5d).

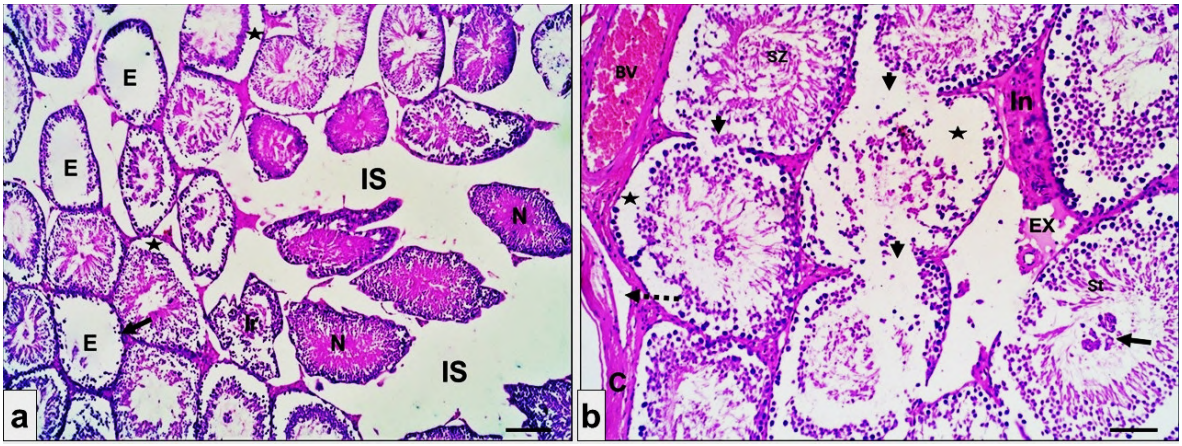

Fig. 4.- Testicular tissue of a rat from the Pestban-treated group showing **(a):** The testicular parenchyma shows loss of interstitial spaces (IS). Varied components of seminiferous tubules; either normal (N), irregularly distributed tissues (Ir), or empty (E) with linear germinal cells inning the basement membrane (short arrow). Some show the separation of germinal cells (star). **(b):** The testicular parenchyma is lined by a thick capsule (C), subscapular separation (detached arrow), and very dilated subscapular blood vessels (BV). The seminiferous tubules show destruction of their basement membranes (arrowheads), empty space (star), collected germinal cells at the center (short arrow), and spermatids near the center (St). notice infiltration (In) and exudation (EX) in the interstitial tissues. H&E staining. Scale bars: a = 40 µm (x200) and b = 20 µm (x400).

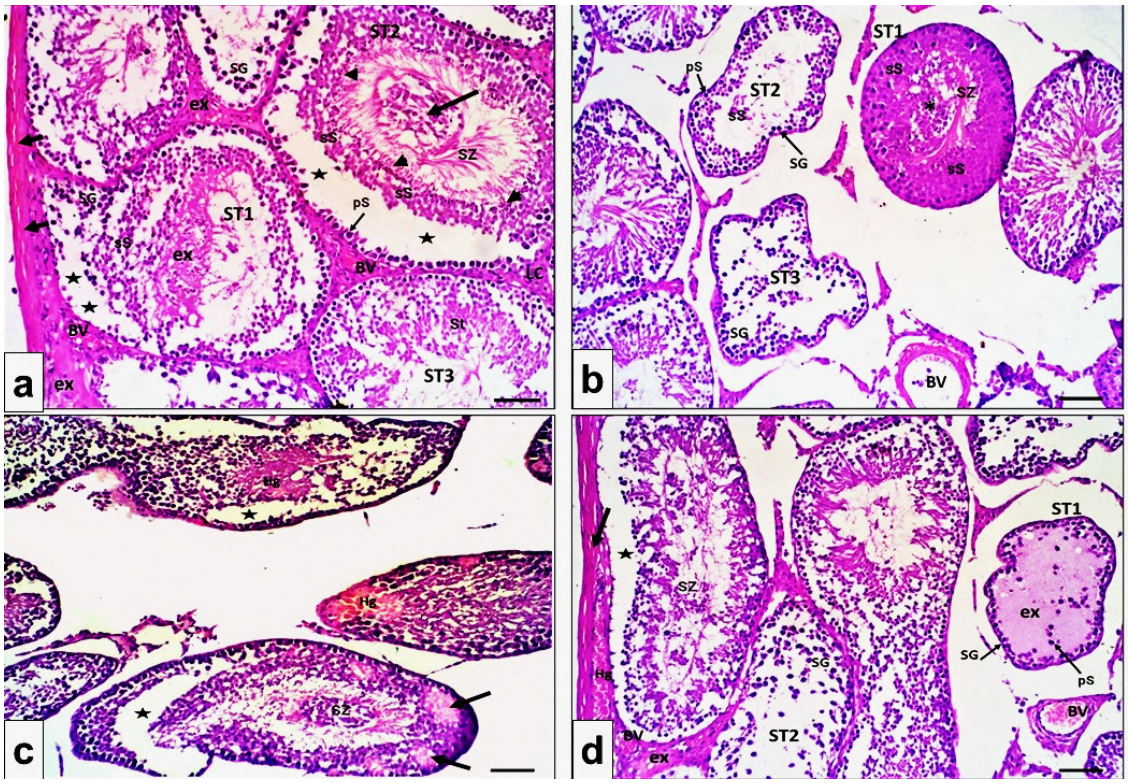

Fig. 5.- Testicular tissue of a rat from the combined Pestban-and-Cyfluthrin-treated group showing **(a):** The testicular parenchyma lined by a very thick capsule (short arrows), subscapular separation (detached arrow) with exudation(ex) and congested blood vessels (BV) of subcapsular area. The interstitial tissues showed exudation (ex), congested and dilated blood vessels (BV) with Leydig cells (LC). The seminiferous tubules show the separation of the germinal cell (star). The seminiferous tubule (ST1) shows condensed spermatogonia (SG), irregular secondary spermatocytes (sS), and exudation(ex). (ST2) shows enlarged primary spermatocytes (Ps) with pericellular space (arrow), linear arranged secondary spermatocytes (sS), small spermatid (arrowheads), spermatozoa (sz) with a central collection of different germ cells (long arrow). (ST3) appears normal. **(b):** Varied seminiferous tubules. (ST1) shows condensed rows of secondary spermatocytes (sS), linear & little spermatozoa (sz) with centrally located germinal cells (*). (ST2) shows enlarged spermatogonia (SG) and primary spermatocytes (pS) with little secondary spermatocytes (sS). (ST3) shows enlarged spermatogonia (SG). Notice enlarged blood vessels (BV). **(c):** The seminiferous tubules show intralaminar hemorrhages (Hg), separation of germinal cells away from the basement membrane (star), and necrotic areas (arrows). **(d):** the section shows thickened capsule (arrow) with subscapular hemorrhage (Hg), dilated blood vessels (BV) and exudation of interstitial tissues. The subscapular seminiferous tubule shows a separation of the germinal cell (star) with condensed spermatozoa in the center (SZ). The seminiferous tubule (ST1) shows intraluminal exudation (ex), and enlarged spermatogonia (SG) with few and enlarged primary spermatocytes (pS). (ST2) shows enlarged & widespread spermatogonia (SG). H&E staining. Scale bars = 20 µm (x400).

PAS staining

The control-group rats showed normal testicular morphology with PAS-positive germ cells and basement membranes of all seminiferous tubules (Fig. 6a). The CYF-treated group showed dense PAS stain of interstitial tissues with destructed basement membrane and separated germ cells (Fig. 6b). The PES-treated group showed mild positive PAS stain in the basement membrane of tubules, and some parts showed destruction (Fig. 6c). The combined PES- and CYF-treated groups showed a very light PAS stain and loss of greater parts of the basement membrane of seminiferous tubules, with few and irregularly distributed germinal cells (Fig. 6d).

Immunohistochemical results

The control groups showed strong positive cytoplasmic brown stains with Melan-A mainly in the interstitial cells of Leydig and in some myoid cells (Fig. 7a). The Cyfluthrin-treated group showed moderate brown stain in some intact interstitial cells of Leydig, but abnormally collected cells Leydig cells showed a negative stain (Fig. 7b). The Pestban-treated group showed a faint brown stain in the interstitial cells of Leydig, in the Sertoli cells and in the myoid cells (Fig. 7c). The combined Pestban-and-Cyfluthrin-treated group showed faint and linear brown staining in the damaged Leydig cells (Fig. 7d). The significant differences between the study groups were presented in Chart 3.

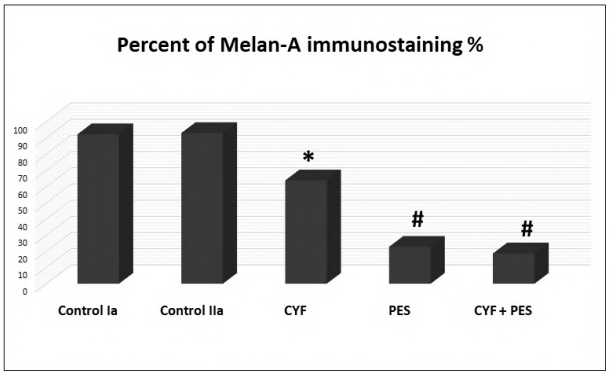

Chart-3 showing; the percent of Melan-A immunostaining in the study groups. * $p < 0.005$ vs control groups. # $p < 0.001$ vs other groups

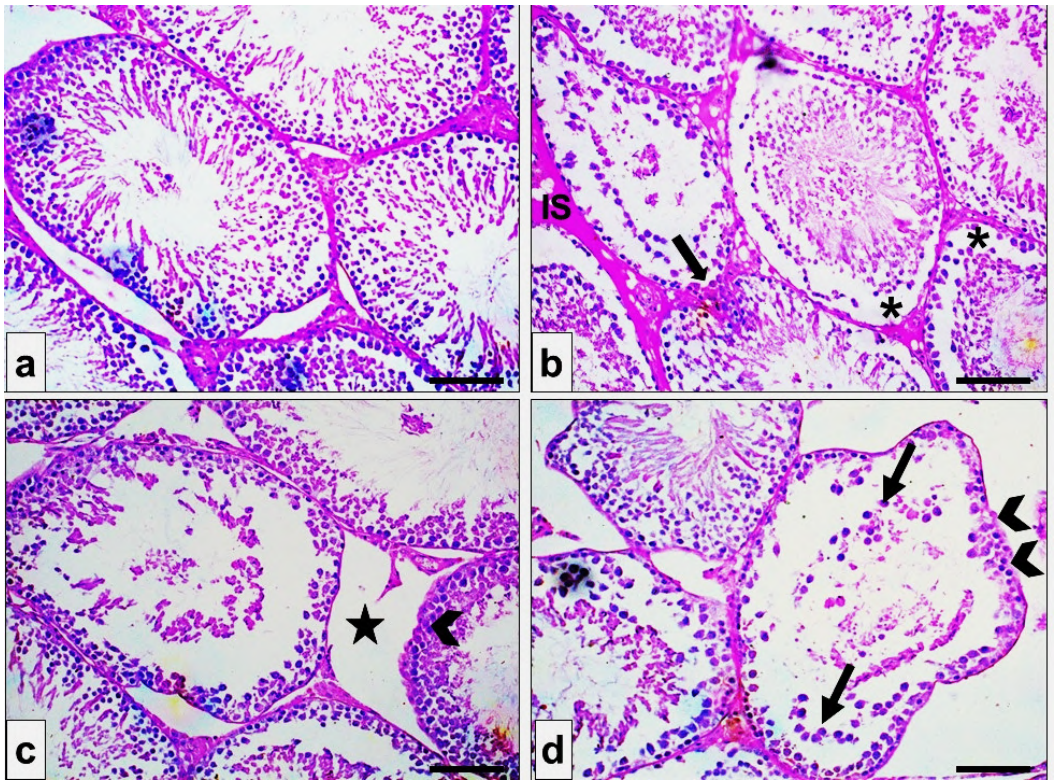

Fig.6. Light microscopy of testicular tissue in different groups stained with periodic acid-Schiff (PAS). (a) Control rat, showing normal testicular morphology with PAS-positive of germ cells and basement membranes of all seminiferous tubules. (b) Cyfluthrin-treated group shows dense PAS stain of interstitial tissues (IS), destructed basement membrane (thick arrow) with separated germ cells (*). (c) Pestban treated group shows mild positive PAS stain of the basement membrane of tubules and some parts showed destruction (arrowhead). (d) combined Pestban-and-Cyfluthrin-treated group shows very light PAS stain with loss of greater parts of the basement membrane of seminiferous tubules (arrowheads) with little and irregularly distributed germinal cells (arrows). PAS staining. Scale bars = 20 µm (x400).

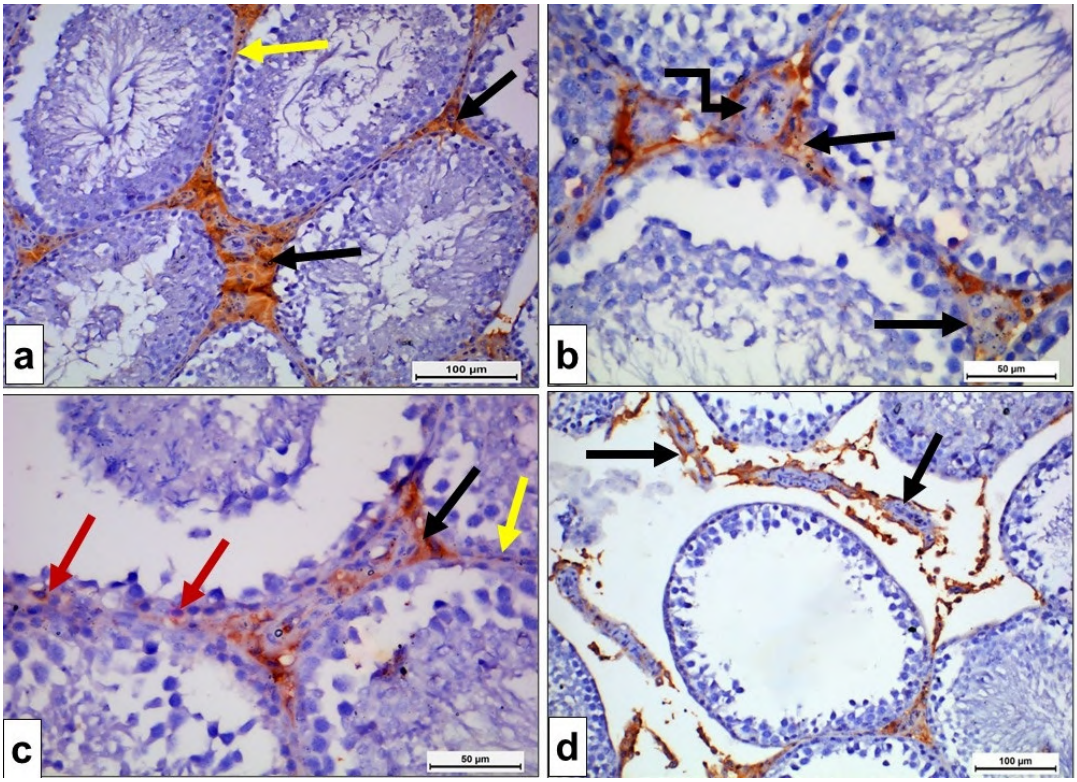

Fig. 7.- Rat testicular tissue of different groups, immuno-histochemical stained with anti-Melan-A. **(a):** The control group shows strong positive cytoplasmic brown stain mainly in the interstitial cell of Leydig (black arrows) and in some myoid cells (yellow arrow). **(b):** Cyfluthrin treated group shows moderate brown stain in some intact interstitial cells of Leydig (arrow), but abnormally collected cells (elbow arrow) showed negative stain. **(c):** Pestban treated group shows a faint brown stain in the interstitial cell of Leydig (black arrow), in the Sertoli cells (red arrows), and in myoid cells (yellow arrow). **(d):** combined Pestban- and-Cyfluthrin-treated group shows faint and linear brown staining in the damaged Leydig cells. (Immunohistochemical staining of anti-Melan-A). Scale bars: a,d = 100 µm; b,c = 50 µm.

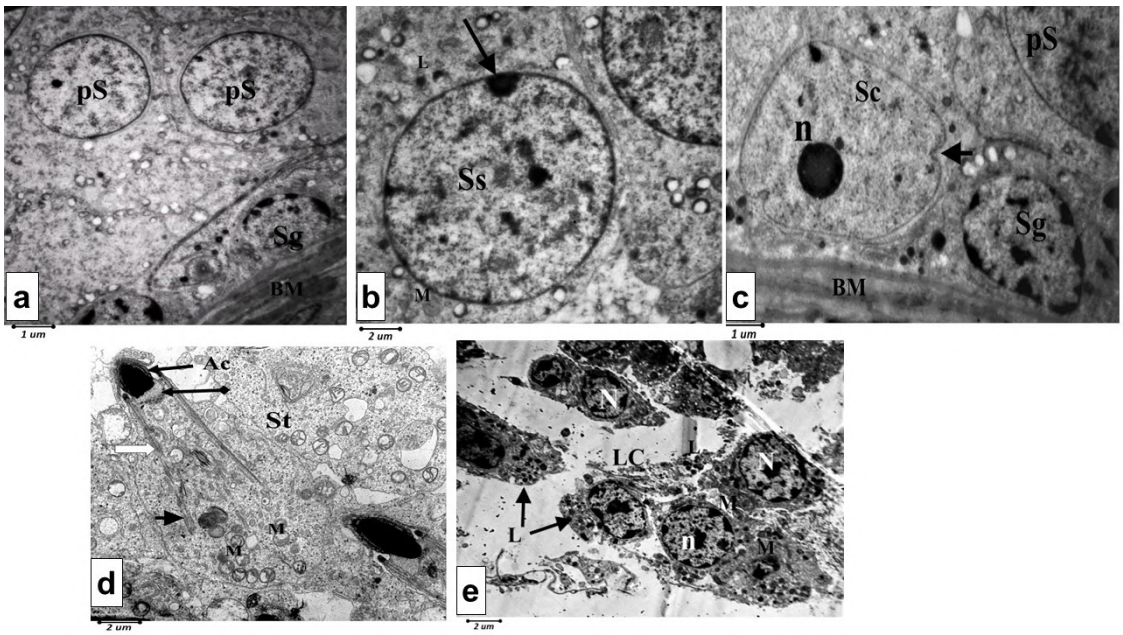

Fig. 8.- Electron micrographs of the control group rat's testis. **(a):** Spermatogonia (Sg) contains a rounded nucleus with peripheral heterochromatin clumps resting on a regular basement membrane (BM), Primary spermatocytes (Ps) with rounded nuclei. **(b):** Secondary spermatocyte (Ss) with large rounded nuclei with heterochromatin clump at one pole (arrow). It is surrounded by mitochondria (M) and lysosomes (L). **(c):** Sertoli cell (Sc) has a pale euchromatic nucleus with prominent nucleolus (n) and shows small nuclear enfolding (arrowhead). Notice spermatogonia (Sg) resting on the basement membrane (BM), with part of primary spermatocytes (Ps). **(d):** Spermatid (St) is composed of a head with an acrosomal cap (AC), middle piece (pointed arrow), cytoplasmic vacuoles (white arrow), annulus (arrowhead), and excess mitochondria (M). **(e):** Leydig cells (LC) showing euchromatic nuclei (N) with peripheral heterochromatin with euchromatic nucleolus (n). Their cytoplasm contains mitochondria (M) and lipid droplets (L). Scale bars: a,c = 1 µm; b,d,e = 2 µm.

Electron microscopic results

Electro micrographs of the control rat's testis showed spermatogonia with rounded nuclei and peripheral heterochromatin clumps resting on a regular basement membrane. The Primary spermatocytes had rounded nuclei (Fig. 8a), while the secondary spermatocyte showed large rounded nuclei with heterochromatin clump at one pole (Fig. 8b). The Sertoli cell showed a pale euchromatic nucleus and prominent nucleolus with small nuclear enfolding (Fig. 8c). The Spermatid was composed of a head with an acrosomal cap, middle piece, annulus, and excess mitochondria (Fig. 8d). Leydig cells showed euchromatic nuclei with peripheral heterochromatin and euchromatic nucleolus; their cytoplasm contained mitochondria and lipid droplets (Fig. 8e).

The Cyfluthrin-treated group (II) showed that the Sertoli cell had a pale euchromatic nucleus with very small nucleolus, and showed large nuclear enfolding lying nearer the thick basement membrane (Fig. 9a). The spermatogonia was elongated, had dark peripheral heterochromatin, and rested on a thick basement membrane; its cytoplasm contained enlarged mitochondria (Fig. 9b). The secondary spermatocyte nucleus showed irregular dense chromatin and an electron-dense body at its periphery, and its cytoplasm contained enlarged rough endoplasmic reticulum (Fig. 9c). The spermatid was composed of an enlarged irregular nucleus and a thin elongated acrosomal cap with residual filaments in front of it. Its cytoplasm contained enlarged mitochondria. Part of the sperm flagellum was surrounded by a huge cytoplasm (Fig. 9d). Differently shaped Leydig cells were noticed, either with oval nuclei, elongated with a small nucleus, or irregularly showing peripheral euchromatin with distributed chromatin. Their cytoplasm contained few lipid droplets (Fig. 9e).

The Pestban-treated group (III) showed pale and irregular Sertoli cells with a euchromatic nucleus, small nucleolus, and too large nuclear enfolding (Fig. 10a). The primary spermatocyte was enlarged, oval, and surrounded by polar perinuclear space. Its cytoplasm contained shrunken mitochondria. The spermatogonia had an enlarged oval-shaped nucleus with a linear collection of

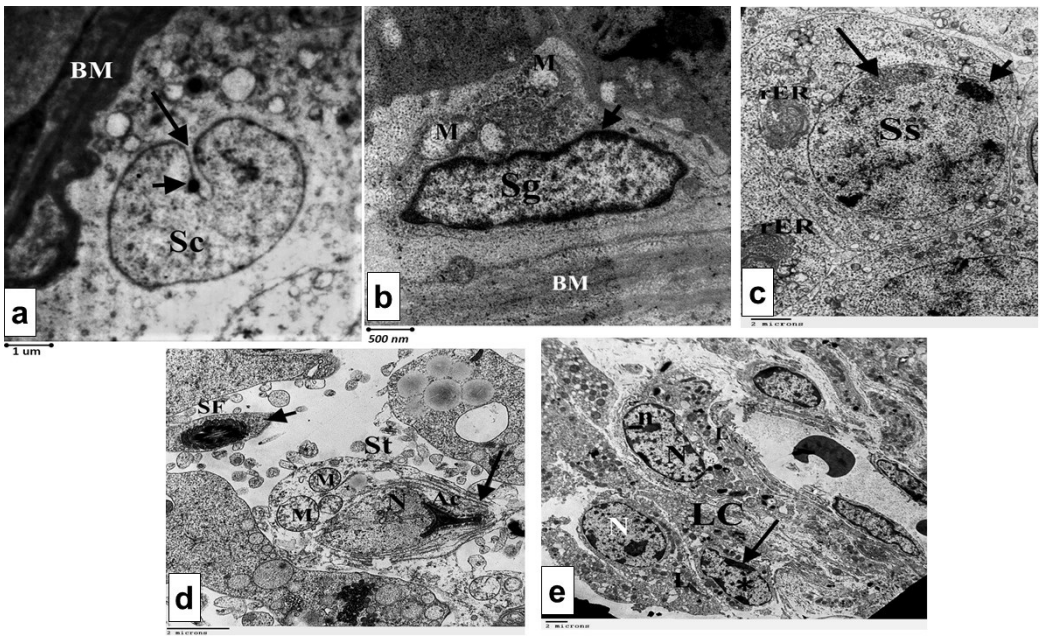

Fig. 9.- Electron micrographs of the testis of Cyfluthrin-treated group. **(a):** Sertoli cell (Sc) has a pale euchromatic nucleus with very small nucleolus (arrowhead) and shows large nuclear enfolding (arrow) and lies nearer to a thick basement membrane (BM). **(b):** elongated Spermatogonia (Sg) with dark peripheral heterochromatin (arrowhead) and resting on thick basement membrane (BM). Its cytoplasm contains enlarged mitochondria (M). **(c):** Secondary spermatocyte (Ss) containing irregular dense chromatin (arrow) and electron-dense body at the periphery of the nucleus (arrowhead). Its cytoplasm contains enlarged rough endoplasmic reticulum (rER). **(d):** Round spermatid (St) composed of enlarged & irregular nucleus (N), thin & elongated acrosomal cap (AC) with residual filaments in front it (arrow). Its cytoplasm contains enlarged mitochondria (M). Part of sperm flagellum (SF) surrounded by huge cytoplasm (arrowhead) **(e):** Different shaped Leydig cells (LC) either oval nucleus (white N), elongated (black N) with small nucleus (n) or irregular showing peripheral euchromatin (arrow) with distributed chromatin (*). Their cytoplasm contains few lipid droplets (L). Scale bars: a = 1 µm; b = 500 nm; c,d,e = 2 µm.

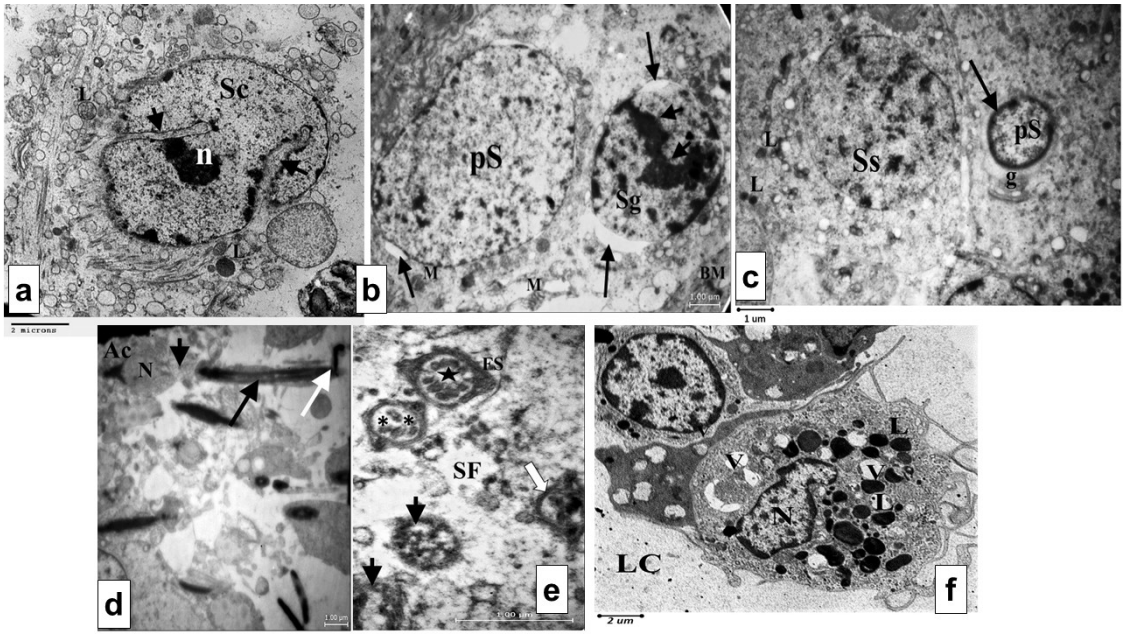

Fig. 10.- Electron micrographs of the testis of Pestban-treated group. **(a):** Sertoli cell (Sc) has a pale, irregular, and euchromatic nucleus with small nucleolus (n) and shows two large nuclear enfoldings (arrowheads). **(b):** Primary spermatocyte (pS) appears enlarged, oval in shape, and surrounded by polar perinuclear space (arrow). Its cytoplasm contains shrunken mitochondria (M). Spermatogonia (Sg) with enlarged and oval-shaped nucleus and resting on basement membrane (BM). It shows a linear collection of dense chromatins (arrowheads), also surrounded by polar perinuclear space (arrow). **(c):** Shrunken primary spermatocyte (pS) nucleus with a dark euchromatic edge (arrow) and surrounded by enlarged Golgi apparatus (g). Secondary spermatocyte (Ss); that's its cytoplasm contains excess lysosomes (L). **(d):** Long spermatid composed of a head with a small nucleus (N), acrosomal cap (Ac), degenerated middle piece (arrowhead), and very thick flagellum (black arrow) with the turned end (white arrow). **(e):** sperm flagellum with wide central vacuole (star) and thick polar fibrous sheath (FS), or with multiple internal vacuoles (*). Notice completely necrosed flagellum (arrowheads) or with thick rim with loss of internal structures (white arrow). **(f):** Leydig cell (LC) with irregular nucleus (N). its cytoplasm contains few lipid droplets (white L), excess (lysosomes (black L), and many vacuoles (V). Scale bars: a,f = 2 µm; b,c,d,e = 1 µm.

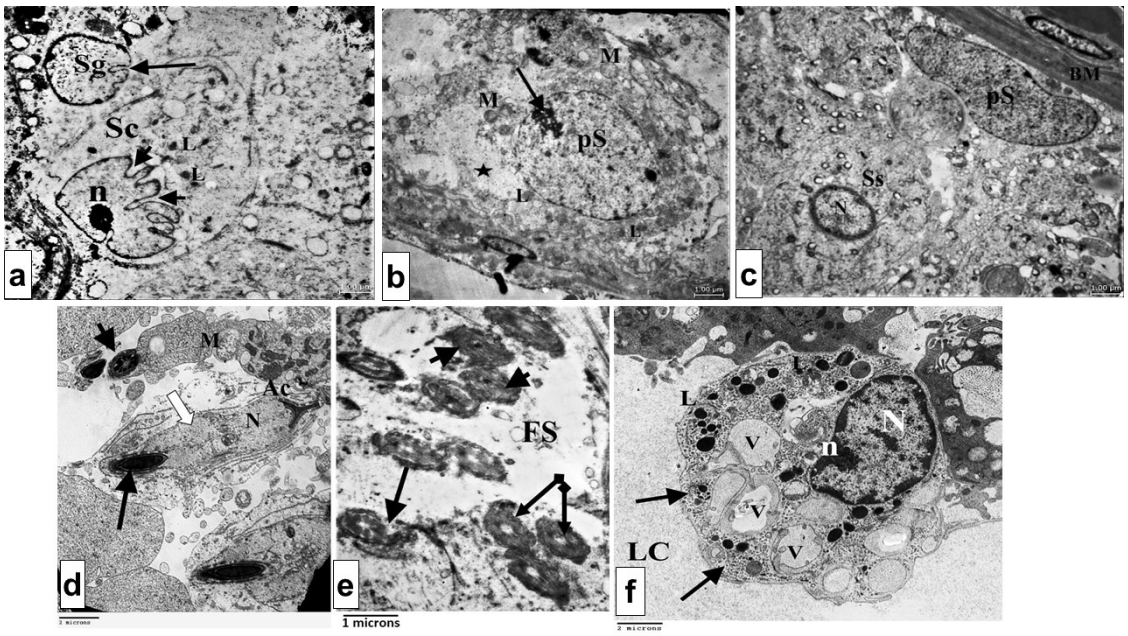

Fig. 11.- Electron micrographs of the testis of the combined Pestban-and-Cyfluthrin-treated group. **(a):** spermatogonia (Sg) which show dark euchromatic rim at one pole and nuclear infoldings at another pole (arrow). Sertoli cell (Sc) has an irregular nucleus with a small nucleolus (n) and shows many nuclear infoldings (arrowheads). Its cytoplasm contains a lot of lysosomes (L). **(b):** Primary spermatocyte (pS) with chromatin clumps at the periphery of the nucleus (arrow). Its cytoplasm shrunken mitochondria (M), lysosomes (L), and empty space (star). **(c):** Primary spermatocyte (pS) with long and euchromatic nucleus. Secondary spermatocyte (Ss); with shrunken nucleus (N). **(d):** abnormal spermatid with enlarged nucleus (N), huge middle piece (white arrow), and thick flagellum (arrow). **(e):** different sperms flagellum (SF) either completely fibrosed fibrous sheath (arrowheads)) or very thick with a small central hole (pointed arrow) or with destructed rim (arrow). **(f):** Leydig cell (LC) with nearly oval nucleus (N) and small polar nucleolus (n). Its cytoplasm contains lipid droplets (L), excess vacuoles (V), and deposited dense particles (arrows). Scale bars: a,b,c,e = 1 µm; d,f = 2 µm.

dense chromatins, also surrounded by polar perinuclear space (Fig. 10b), shrunken primary spermatocyte nucleus with dark euchromatic edge and surrounded by enlarged Golgi apparatus. The cytoplasm of the secondary spermatocyte contained excess lysozymes (Fig. 10c). The spermatid was composed of the head with a small nucleus, acrosomal cap, degenerated middle piece, and very thick flagellum with a turned end (Fig. 10d). The sperm flagellum showed a wide central vacuole and a thick polar fibrous sheath, sometimes completely necrosed (Fig. 10e). The Leydig cells showed an irregular nucleus, and their cytoplasm contained few lipid droplets, excess lysosomes, and many vacuoles (Fig. 10f)**.**

The testicular tissues of the combined Pestban-and-Cyfluthrin-treated group (IV) showed the spermatogonia with a dark euchromatic rim at one pole and nuclear infoldings at another pole. The Sertoli cell owned numerous nuclear infoldings, small, irregular nuclei, and a large number of lysosomes in its cytoplasm (Fig. 11a). The nucleus of the primary spermatocyte displayed chromatin aggregates at its perimeter, and its cytoplasm displayed vacuolations, lysosomes, and reduced mitochondria (Fig. 11b). The nucleus of the secondary spermatocyte was small (Fig. 11c). All of the spermatids in this group had abnormally thick flagella with a variety of defects, including either a totally thickened fibrous sheath or a very thick flagellum with a small central hole (or with a destroyed rim) (Fig. 11d, e). The Leydig cells displayed a tiny polar nucleolus and an oval nucleus. Lipid droplets, extra vacuoles, and deposited dense particles were noticed in their cytoplasm (Fig. 11f).

DISCUSSION

Reproductive health is gradually deteriorating due to multiple endogenous and exogenous factors, such as environmental pollutants and endocrine disruptors, including pesticides (Singh et al., 2014). Over the previous decades, male infertility has obtained pronounced interest worldwide. The diminished sperm concentration is an exceptional problem which has appeared in the European and African populations in the last 50 years (Zhang et al., 2021).

Pesticide toxicity is occasionally constrained to single chemical exposure. However, people are usually subjected to different chemicals in their daily activities. This blended and mixed exposure can result in deteriorating health effects (Rani et al., 2021). In the present study, we tried to investigate reproductive toxicity triggered by single and mutual exposure to CYF and PES. Oral dosing of CYF, PES, and their combination for 60 days in our study triggered a significant decrease in the body weight and testis weight when compared to the control group, which agreed with previous research that studied mixtures of different pesticides (Wang et al., 2009; Sf et al., 2011; Abdel-Rahim et al., 2014)**.**

Authors have suggested that the decreased body weight gain might be due to anorexia and associated lowering of food intake. Also, Iyyadurai et al. (2014) and Rajawat et al. (2014**)** reported a significant reduction in body weight of CYF-treated rats, due to its cytotoxic effect on somatic cells with direct cytotoxic action of PYR insecticide on the testicular tissues.

This theory was supported by others (Ghorbani-Taherdehi et al., 2020)**.** They explained that OP and PYR exposure resulted in regressive and necrotic testicular changes, in addition to decreasing the germ cell numbers and spermatozoa. Alaa-Eldin et al. (2017) reported that a decrease in testicular weight might be directly related to reduced serum testosterone, FSH, and LH levels, as observed in the current study.

In the present study, the mean values of serum testosterone, follicle-stimulating hormone (FSH), and luteinizing hormone (LH) levels in CYF group and PES group decreased significantly. Rats in combined treated group displayed highly significant declines.

The results of the current study coincided with Zidan (2008)**,** who reported that OP exposure at different doses could reduce testosterone levels. Kang et al. (2004) discussed that decreased testosterone level was associated with defects in gonads and suppression of LH and FSH levels**.** Kitamura et al. (2003) explained that PES could act as androgen receptor antagonists or suppress genes related to hypothalamic gonadotropin synthesis

(LH and FSH) or steroidogenesis. Sharma et al. (2005) reported similar results after exposure to PYR. Joshi et al. (2003) explained that lowering reproductive hormones in male rats suggests extra-testicular targets of PYR. CYF may influence the hypothalamus-pituitary axis. LH stimulates Leydig cells to produce testosterone; hence, a decrease in LH may be also a contributing factor to the low level of testosterone. PYR pesticides pose anti-gonadal action or deprived levels of androgens that resulted in decreased levels of male gonadal hormones, mitochondrial membranes alteration and damage in Leydig cells, down-regulating expression of gene signaling for essential proteins, and decreased sperm health.

In the present study, oxidative stress load (MDA) in individually CYF- and PES-treated rats showed a significant increase compared with the control group, while they significantly increased in CYF+PES-treated group showed highly significant increases compared to other groups. Various studies regarding OP including PES-induced oxidative stress in diverse tissues bolstered the results of current studies (Nurulain et al., 2013).

Exposure to broad OP pesticides from different sources builds indices of oxidative stress in cells, animals, and humans. These pesticides raise the production of ROS and stimulate alterations in endogenous antioxidant enzymes leading to free radical-mediated lipid peroxidation. In addition to declined antioxidant capacity, free radical-mediated DNA damage, and lipid peroxidation (Pearson and Patel, 2016).

During PYR metabolism, reactive oxygen species (ROS) are produced, leading to oxidative stress. Excess production could have damaging effects on cell membranes in the testes (Stewart et al., 2016). Our results were similar to Martínez et al. (2019), who reported that CYF induced a significant ROS generation, and lipid peroxides presented as malondialdehyde.

The results of the present study for sperm analysis revealed that single pesticide treatments significantly reduced sperm motility, viability, and count, whereas sperm head abnormalities increased significantly. Also, rats in the combined group showed the highest significant difference when compared with those of other groups. These results agreed with Farag et al. (2010), who reported that CPF oral gavage showed marked decrease in sperm count, motility, and an increased percentage of abnormal forms. Sperm count reduction observed in the present study may be directly related to decreased serum testosterone level leading to gradual inhibition of the spermatogenesis process or due to low FSH and LH levels (Sharma et al., 2005). Moreover, reduced sperm motility could be attributed to distressed mitochondrial and intracellular ATP activity, altered fructose synthesis, and attrition of spermatozoan microtubule structure in pesticide-treated rats (Heikal et al., 2014). In accordance with our results, Prakash et al. (2010) explained that Cypermethrin administration led to enzymatic alterations in testes as well as disruption of testosterone synthesis. These changes may cause abnormal sperms leading to complete male sterility.

Yousef et al. (2003) suggested that PYR-induced male reproductive toxicity through a hormone-disrupting mechanism and a neuro-endocrine-mediated phenomenon. PYR interacts competitively with androgen receptors and sex hormone-binding globulin disrupting the endocrine system by mimicking the effect of the female hormone estrogen, leading to low sperm counts. Also, PYR exposure could evoke reactive oxygen species production and subsequently DNA damage, which adversely affects sperm motility and viability, and increases abnormal forms (Bian, 2004). Oxidative damages associated with PYR could mainly affect both Sertoli and Leydig cells. Sertoli cells are accountable for supporting developing germ cells. So, sperm motility would be expected to decline following a decrease in serum testosterone concentration (Stewart et al., 2016).

According to the results of the present study, histological damage was observed in individually treated groups (II) and (III), but it was pronounced in mutual treatment in the combined group.

These results agreed with Rajawat et al. (2014), who stated that CYF caused varied testicular histopathological damage. For example, the germinal epithelium showed shrunken and broken areas, seminiferous tubules were displaced, and the luminal diameter became narrower with widening

the interstitial spaces. Also, our results matched with Dohlman et al. (2016), pointing to cellular damage following CYF exposure due to oxidative stress.

Our findings coincided with Kalender et al. (2012), who reported degeneration, necrosis, and decreased spermatogenic cells in some seminiferous tubules of CPF-treated rats (main constitutes of PES). Mosbah et al.(2016) observed a total loss of germinal cells (all the stages) with severe degeneration of seminiferous tubules.

The testicular changes in the current study following PES exposure could be referred to its ability to generate oxidative stress in different tissues and organs, leading to oxidative damage and deleterious pathological changes in the testis (Farag et al., 2010). It has been documented that OP compounds can cross the blood-testis barrier and directly degenerate the spermatogenic and Leydig cells (Uzun et al., 2009).

The histopathological observations in the CYF group were near the results by Elbetieha et al. (2001), who studied the toxic effects of some synthetic PYR (cypermethrin). They found a significant reduction in seminiferous tubule cell layers, with excessive histopathological changes. Ahmad et al. (2012) noted spermatogenesis inhibition with giant cell formation related to disturbed steroidogenesis induced by cypermethrin exposure.

Our electron microscopic results revealed obvious damage in the cytoplasmic organelles in most cells of the seminiferous tubules in the rats individually and co-treated with CYF and PES, which point to functional changes of these cells. According to Joshi et al. (2011), mitochondria are the vital organelles representing cellular damage, and pesticide-derived mitochondrial pathologies are well known.

Spermatid organelles abnormalities found in the combined CYF-and-PES-treated group in our results were similar to those reported by Iwan and Golec, (2020), who observed a significant reduction in intraluminal sperm concentrations following PYR treatment.

El-Gerbed (2013) stated that pesticides were classified as the foremost toxic chemicals that target Sertoli cells. It was assumed that the Sertoli cells facilitate all metabolic exchange with the systemic compartment. The present ultrastructural study revealed marked damage to the Sertoli cell components in the combined group.

Our immunohistochemical results using Melan-A were in accordant with Zhang et al. (2017) who focused on the role of oxidative stress on the viability and functions of the Leydig cells. Similarly, Shojaeepour et al. (2021) used Melan-A to investigate the possible role of Sertoli cells in processing the routes of Cadmium-induced testicular injury. Sertoli cells gathered and produced multinucleated giant cells in the seminiferous tubules throughout the atrophic process, which could be dependent upon Sertoli cells viability and function.

Sertoli cells play supportive and nourishing roles for germ cells in seminiferous tubules. So, they are involved in testis formation and spermatogenesis. Melan-A is considered one of the important markers more expressed by Sertoli cells (Meroni et al., 2019).

In conclusion, when considering the results for different PYR, including CYF studies, researchers found that all PYR types damaged the reproductive system of adult males. All the following parameters are inversely affected by PYR exposure: testis weight, sperm count, sperm morphology, sperm motility, and serum testosterone level, all are inversely affected (Zhang et al., 2018). OP and PYR co-exposure led to an excess reduction in reproductive organs' weight and a lower level of sex hormones (testosterone, FSH, and LH) than each pesticide alone, which was confirmed by histological and ultrastructural disorganization of the testis. Organophosphate pesticides can cross the blood–testicular barrier and cause degeneration of the spermatogenic epithelium and Leydig cells (Moreira et al., 2021).

Abd-Elhakim et al. (2021) recorded a synergistic outcome between two pesticides' (OP and PYR) co-exposure in almost all estimated parameters. Synergism and potentiation observed in the current study could be associated with ROS excess generation inducing more suppression of an essential silent information regulator type-1/ telo-

merase reverse transcriptase (TERT), and peroxisome proliferator-activated receptor gamma coactivator 1-alpha (PGC-1α) pathway to give rise to this synergistic effect. In this condition, Ma et al. (2019) stated that mixing or co-administration of pesticides that have androgenic antagonistic prosperities could act mutually, especially at the receptor level.

CONCLUSION

The present study indicated that single and mixed exposure to Cyfluthrin and Pestban had deleterious effects on the male reproductive system that could induce infertility. They impaired reproductive functions through abnormal reproductive parameters such as sperm count and viability. The testicular structural and ultra-structural outcomes confirmed the severely impaired and apoptotic germ cells. These findings were more prominent in co-exposure.

REFERENCES

ABD-ELHAKIM YM, EL SHARKAWY NI, EL BOHY KM, HASSAN MA, GHARIB HSA, EL-METWALLY AE, ARISHA AH, IMAM TS (2021) Iprodione and/or chlorpyrifos exposure induced testicular toxicity in adult rats by suppression of steroidogenic genes and SIRT1/TERT/PGC-1α pathway. *Environ Sci Pollut Res*, 28: 56491-56506.

ABDEL-RAHIM EA, ABDEL-MOBDY YE, ALI RF, MAHMOUD HA (2014) Hepatoprotective effects of solanum nigrum linn fruits against cadmium chloride toxicity in albino rats. biol. *Trace Elem Res*,160: 400-408.

ADAMKOVICOVA M, TOMAN R, MARTINIAKOVA M, OMELKA R, BABOSOVA R, KRAJCOVICOVA V, GROSSKOPF B, MASSANYI P (2016) Sperm motility and morphology changes in rats exposed to cadmium and diazinon. *Reprod Biol Endocrinol*, 14: 42.

AHMAD L, KHAN A, KHAN MZ (2012) Pyrethroid induced reproductive toxico-pathology in non-target species. *Pak Vet J Pak*, 32: 1-9.

AINI N, SUSTRIAWAN B, WAHYUNINGSIH N, MELA E (2022) Blood sugar, haemoglobin and malondialdehyde levels in diabetic white rats fed a diet of corn flour cookies. *Foods*, 11: 1819.

ALAA-EL-DIN EA, EL-SHAFEI DA, ABOUHASHEM NS (2017) Individual and combined effect of chlorpyrifos and cypermethrin on reproductive system of adult male albino rats. *Environ Sci Pollut Res*, 24: 1532-1543.

ALAA EL-DIN E, ABDALLAH AA, ABDALLAH EL-SHAFEI D, ABOUHASHEM N, MOSTAFA H (2022) Individual and mixture effect of Deltamethrin and Dimethoate on liver: A biochemical, histopathological, immuno-histochemical, and genotoxic study. *Egypt J Forensic Sci Appl Toxicol*, 22: 23-38.

BIAN Q (2004) Study on the relation between occupational fenvalerate exposure and spermatozoa DNA damage of pesticide factory workers. *Occup Environ Med*, 61: 999-1005.

CHEN L, WANG R, WANG W, LU W, XIAO Y, WANG D, DONG Z (2015) Hormone inhibition during mini-puberty and testicular function in male rats. *Int J Endocrinol Metab*, 13(4): e25465.

DOHLMAN TM, PHILLIPS PE, MADSON DM, CLARK CA, GUNN PJ (2016) Effects of label-dose permethrin administration in yearling beef cattle: I. Bull reproductive function and testicular histopathology. *Theriogenology*, 85: 1534-1539.

ELBETIEHA A, DA'AS SI, KHAMAS W, DARMANI H (2001) Evaluation of the toxic potentials of cypermethrin pesticide on some reproductive and fertility parameters in the male rats. *Arch Environ Contam Toxicol*, 41: 522-528.

EL-GERBED MS (2013) Histopathological and ultrastructural effects of methyl parathion on rat testis and protection by selenium. *J Appl Pharm Sci*, 3: S53-S63.

ENSAFI AA, KHAYAMIAN T, HASANPOUR F (2008) Determination of glutathione in hemolysed erythrocyte by flow injection analysis with chemiluminescence detection. *J Pharm Biomed Anal*, 48: 140-144.

FARAG AT, RADWAN A H, SOROUR F, EL OKAZY A, EL-AGAMY E, EL-SEBAE AE (2010) Chlorpyrifos induced reproductive toxicity in male mice. *Reprod Toxicol*, 29: 80-85.

GHORBANI-TAHERDEHI F, NIKRAVESH MR, JALALI M, FAZE A, GORJI VALOKOLA M (2020) Evaluation of the anti-oxidant effect of ascorbic acid on apoptosis and proliferation of germinal epithelium cells of rat testis following malathion-induced toxicity. *Iran J Basic Med Sci*, 23: 569-575.

HAMOUD A (2019) Possible role of selenium nanoparticles on gentamicin-induced toxicity in rat testis: Morphological and morphometric study. *Egypt J Histol*, 42: 861-873.

HEIKAL TMH, MOSSA AT, IBRAHIM AW, ABDEL-HAMI HF (2014) Oxidative damage and reproductive toxicity associated with cyromazine and chlorpyrifos in male rats: the protective effects of green tea extract. *Res J Environ Toxicol*, 8: 53-67.

HOŁYŃSKA-IWAN I, SZEWCZYK-GOLEC K (2020) Pyrethroids: how they affect human and animal health? *Medicina (Mex.)*, 56: 582.

HSU YC (2015) Theory and practice of lineage tracing. *Stem Cells*, 33: 3197-3204.

IYYADURAI R, PETER JV, IMMANUEL S, BEGUM A, ZACHARIAH A, JASMINE S, ABHILASH KP (2014) Organophosphate-pyrethroid combination pesticides may be associated with increased toxicity in human poisoning compared to either pesticide alone. *Clin Toxicol*, 52: 538-541.

JOSHI SC, MATHUR R, GAJRAJ A, SHARMA T (2003) Influence of methyl parathion on reproductive parameters in male rats. *Environ Toxicol Pharmacol*, 14: 91-98.

JOSHI SC, BANSAL B, JASUJA, ND (2011) Evaluation of reproductive and developmental toxicity of cypermethrin in male albino rats. *Toxicol Environ Chem*, 93: 593-602.

KALENDER Y, KAYA S, DURAK D, UZUN FG, DEMIR F (2012) Protective effects of catechin and quercetin on antioxidant status, lipid peroxidation and testis-histoarchitecture induced by chlorpyrifos in male rats. *Environ Toxicol Pharmacol*, 33: 141-148.

KAMANDE DS, ODUFUWA OG., MBUBA E, HOFER L, MOORE SJ (2022) Modified World Health Organization (WHO) tunnel test for higher throughput evaluation of insecticide-treated nets (ITNs) considering the effect of alternative hosts, exposure time, and mosquito density. *Insects*, 13: 562.

KANG HG, JEONG SH, CHO JH, KIM DG, PARK JM, CHO MH (2004) Chlropyrifos-methyl shows anti-androgenic activity without estrogenic activity in rats. *Toxicology*, 199(2-3): 219-230.

KIM S, KWON H, PARK JH, CHO B, KIM D, OH SW, LEE CM, CHOI HC (2012) A low level of serum total testosterone is independently associated with nonalcoholic fatty liver disease. *BMC Gastroenterol*, 12: 69.

KITAMURA S, SUZUKI T, OHTA S, FUJIMOTO N (2003) Antiandrogenic activity and metabolism of the organophosphorus pesticide fenthion and related compounds. *Environ Health Perspect*, 111: 503-508.

KORACEVIC D (2001) Method for the measurement of antioxidant activity in human fluids. *J Clin Pathol*, 54: 356-361.

MA M, CHEN C, YANG G, WANG Y, WANG T, LI Y, QIAN Y (2019) Combined anti-androgenic effects of mixtures of agricultural pesticides using in vitro and in silico methods. *Ecotoxicol Environ Saf*, 186: 109652.

MARTÍNEZ MA, RODRÍGUEZ JL, LOPEZ-TORRES B, MARTÍNEZ M, MARTÍNEZ-LARRAÑAGA MR, ANADÓN A, ARES I (2019) Oxidative stress and related gene expression effects of cyfluthrin in human neuroblastoma SH-SY5Y cells: Protective effect of melatonin. *Environ Res*, 177: 108579.

MERONI SB, GALARDO MN, RINDONE G, GORGA A, RIERA MF, CIGORRAGA SB (2019) Molecular mechanisms and signaling pathways involved in Sertoli cell proliferation. *Front Endocrinol*, 10: 224.

MOHAFRASH SMM, ABDEL-HAMID HF, MOSSA ATH (2017) Adverse effects of sixty days sub-chronic exposure to β-cyfluthrin on male rats. *J Environ Sci Technol*, 10: 1-12.

MOHAMMADI M, SHADNOUSH M, SOHRABVANDI S, YOUSEFI M, KHORSHIDIAN N, MORTAZAVIAN AM (2021) Probiotics as potential detoxification tools for mitigation of pesticides: a mini review. *Int J Food Sci Technol*, 56: 2078-2087.

MOREIRA S, PEREIRA SC, SECO-ROVIRA V, OLIVEIRA PF, ALVES MG, PEREIRA M DE L (2021) Pesticides and male fertility: a dangerous crosstalk. *Metabolites*, 11: 799.

MORGAN AM, EL-ATY AMA (2008) Reproductive toxicity evaluation of pestban insecticide exposure in male and female rats. *Toxicol Res*, 24: 137-150.

MORI K, KAIDO M, FUJISHIRO K, INOUE N, KOIDE O, HORI H, TANAKA I (1991) Dose dependent effects of inhaled ethylene oxide on spermatogenesis in rats. *Occup Environ Med*, 48: 270-274.

MOSBAH R, YOUSEF MI, MARANGHI F, MANTOVANI A (2016) Protective role of Nigella sativa oil against reproductive toxicity, hormonal alterations, and oxidative damage induced by chlorpyrifos in male rats. *Toxicol Ind Health*, 32: 1266-1277.

MOSTAFA HES, ABD EL-BASET SA, KATTAIA AAA, ZIDAN RA, AL SADEK MMA (2016) Efficacy of naringenin against permethrin-induced testicular toxicity in rats. *Int J Exp Pathol*, 97: 37-49.

NAGAYA N, FUJII T, IWASE T, OHGUSHI H, ITOH T, UEMATSU M, YAMAGISHI M, MORI H, KANGAWA K, KITAMURA S (2004) Intravenous administration of mesenchymal stem cells improves cardiac function in rats with acute myocardial infarction through angiogenesis and myogenesis. *Am J Physiol Heart Circ Physiol*, 287: H2670-H2676.

NEMZEK JA, BOLGOS GL, WILLIAMS BA, REMICK DG (2001) Differences in normal values for murine white blood cell counts and other hematological parameters based on sampling site. *Inflamm Res*, 50: 523-527.

NURULAIN S, SZEGI P, TEKES K, NAQVI S (2013) Antioxidants in organophosphorus compounds poisoning. *Arch Ind Hyg Toxicol*, 64: 169-177.

PARRA-ARROYO L, GONZÁLEZ-GONZÁLEZ RB, CASTILLO-ZACARÍAS C, MELCHOR MARTÍNEZ EM, SOSA-HERNÁNDEZ JE, BILAL M, IQBAL, HMN, BARCELÓ D, PARRA-SALDÍVAR R (2022) Highly hazardous pesticides and related pollutants: Toxicological, regulatory, and analytical aspects. *Sci Total Environ*, 807: 151879.

PEARSON JN, PATEL M (2016) The role of oxidative stress in organophosphate and nerve agent toxicity: Redox and organophosphates. *Ann NY Acad Sci*, 1378: 17-24.

PRAKASH N, KUMAR V, SUNILCHANDRA U, PAVITHRA B, PAWAR A (2010) Evaluation of testicular toxicity following short-term exposure to cypermethrin in albino mice. *Toxicol Int*, 17: 18.

RAJAWAT N, SONI I, MATHUR P, GUPTA D (2014) Cyfluthrin-induced toxicity on testes of Swiss albino mice. *Int J Curr Microbiol App Sci*, 3: 334-343.

RANI L, THAPA K, KANOJIA N, SHARMA N, SINGH S, GREWAL AS, SRIVASTAV AL, KAUSHAL J (2021) An extensive review on the consequences of chemical pesticides on human health and environment. *J Clean Prod*, 283: 124657.

SF AMA, AO A, MU K (2011) Protective effect of vitamin C on biochemical alterations induced by subchronic co-administration of chlorpyrifos and lead in Wistar rats. *J Environ Anal Toxicol*, 1: 108.

SHARMA Y, BASHIR S, IRSHAD M, NAG TC, DOGRA TD (2005) Dimethoate-induced effects on antioxidant status of liver and brain of rats following subchronic exposure. *Toxicology*, 215: 173-181.

SHOJAEEPOUR S, DABIRI S, DABIRI B, IMANI M, FEKRI SOOFI ABADI M, HASHEMI F (2021) Histopathological findings of testicular tissue following cadmium toxicity in rats. *Iran J Pathol*, 16: 348-353.

SILVA AM, MARTINS-GOMES C, SILVA TL, COUTINHO TE, SOUTO EB, ANDREANI T (2022) In vitro assessment of pesticides toxicity and data correlation with pesticides physicochemical properties for prediction of toxicity in gastrointestinal and skin contact exposure. *Toxics*, 10: 378.

SINGH R, SHARMA P, HUQ A (2014) Cypermethrin-induced reproductive toxicity in the rat is prevented by resveratrol. *J Hum Reprod Sci*, 7: 99.

STEWART J, SHIPLEY C, IRELAND F, JARRELL V, TIMLIN C, SHIKE D, FELIX T (2016) Long-term effects of pyrethrin and cyfluthrin, a type II synthetic pyrethroid, insecticide applications on bull reproductive parameters. *Reprod Domest Anim*, 51: 680-687.

UZUN FG, KALENDER S, DURAK D, DEMIR F, KALENDER Y (2009) Malathion-induced testicular toxicity in male rats and the protective effect of vitamins C and E. *Food Chem Toxicol*, 47: 1903-1908.

VAN DER HORST G, KOTZÉ SH, O'RIAIN MJ, MAREE L (2019) Testicular structure and spermatogenesis in the naked mole-rat is unique (degenerate) and atypical compared to other mammals. *Front Cell Dev Biol*, 7: 234.

VASAN S (2011) Semen analysis and sperm function tests: How much to test? *Indian J Urol*, 27: 41.

WANG C, CHEN F, ZHANG Q, FANG Z (2009) Chronic toxicity and cytotoxicity of synthetic pyrethroid insecticide cis-bifenthrin. *J Environ Sci*, 21: 1710-1715.

WANG Z, LIU RAN, ZHANG L, YU S, NIE Y, DENG Y, LIU RUI, ZHU W, ZHOU Z, DIAO J (2022) Thermoregulation of Eremias argus alters temperature-dependent toxicity of beta-cyfluthrin: Ecotoxicological effects considering ectotherm behavior traits. *Environ Pollut*, 293: 118461.

YOUSEF MI, EL□DEMERDASH FM, AL□SALHEN KS (2003) Protective role of isoflavones against the toxic effect of cypermethrin on semen quality and testosterone levels of rabbits. *J Environ Sci Health Part B*, 38: 463-478.

ZHANG X, ZHANG T, REN X, CHEN X, WANG S, QIN C (2021) Pyrethroids toxicity to male reproductive system and offspring as a function of oxidative stress induction: Rodent studies. *Front Endocrinol*, 12: 656106.

ZHANG YF, YANG JY, LI YK, ZHOU W (2017) Toxicity and oxidative stress induced by T-2 toxin in cultured mouse Leydig cells. *Toxicol Mech Meth*, 27: 100-106.

ZHANG Z, WU Y, YUAN S, ZHANG P, ZHANG J, LI H, LI X, SHEN H, WANG Z, CHEN G (2018) Glutathione peroxidase 4 participates in secondary brain injury through mediating ferroptosis in a rat model of intracerebral hemorrhage. *Brain Res*, 1701: 112-125.

ZIDAN NEH (2008) Evaluation of the reproductive toxicity of chlorpyrifos methyl, diazinon and profenofos pesticides in male rats. *Int J Pharmacol*, 5: 51-57.